

 Open access • Posted Content • DOI:10.1007/S10904-021-02134-7

Comparison Study of Elastic, Physical and Structural Properties for Strontium Oxide and Manganese Oxide in Borotellurite Glasses for High Strength Glass Application

— [Source link](#) 

Nazirul Nazrin Shahrol Nidzam, Halimah Mohamed Kamari, Muhammad Syaamil Mohd Sukari, Fatin Azira Mohamad Alauddin ...+8 more authors





Institutions: Universiti Putra Malaysia, University of Sfax, King Khalid University, Monash University, Clayton campus ...+2 more institutions

Published on: 03 Nov 2021 - Journal of Inorganic and Organometallic Polymers and Materials (Springer US)

Topics: Strontium oxide, Elastic modulus, Bulk modulus, Amorphous solid and Strontium

Related papers:

- [The effect of manganese \(IV\) oxide doping on the optical and elastic properties of calcium borate glass derived from waste chicken eggshell](#)
- [Effect of yttrium on the physical, elastic, and structural properties of neodymium-doped lead borotellurite glass](#)
- [Elastic properties of TeO₂-ZnO-Ag₂O doped with Nd₂O₃](#)
- [Influence of manganese doping on elastic and structural properties of silica borotellurite glass](#)
- [Physical and elastic properties of TeO₂-Gd₂O₃ glasses: Role of zinc oxide contents variation](#)

Share this paper:    

View more about this paper here: <https://typeset.io/papers/comparison-study-of-elastic-physical-and-structural-37xdvtujp6>

Comparison Study of Elastic, Physical and Structural Properties for Strontium Oxide and Manganese Oxide in Borotellurite Glasses for High Strength Glass Application

NAZIRUL NAZRIN SHAHROL NIDZAM (✉ nazirulnazrin@gmail.com)

Universiti Putra Malaysia

Halimah Mohamed Mohamed Kamari

Universiti Putra Malaysia

Muhammad Syaamil Mohd Sukari

Universiti Putra Malaysia

Fatin Azira Mohamad Alauddin

Universiti Putra Malaysia

Hasnimulyati Laoding

Universiti Teknologi MARA Cawangan Pahang

Imed Boukhris

King Khalid University

Sin Wei Hann

Monash University Clayton Australia

Research Article

Keywords: strontium oxide, manganese oxide, boron oxide, tellurite glass, melt quenching method, elastic measurement

Posted Date: August 4th, 2021

DOI: <https://doi.org/10.21203/rs.3.rs-772802/v1>

License:  This work is licensed under a Creative Commons Attribution 4.0 International License.

[Read Full License](#)

Version of Record: A version of this preprint was published at Journal of Inorganic and Organometallic Polymers and Materials on November 3rd, 2021. See the published version at <https://doi.org/10.1007/s10904-021-02134-7>.

Abstract

In this research the melt quenching technique method was used to synthesize two series of borotellurite glass systems doped with manganese and strontium. Elastic measurement, X-Ray Diffraction and Fourier Transform Infrared spectroscopy were used to characterize the prepared glass samples. The increment of molar volume confirmed the theory that molar volume is inversely proportional to the density parameters. A broad hump appeared in XRD as the samples shown pure amorphous nature. In FTIR, the functional group vibrations of tellurite network were recorded such as TeO_4 trigonal bipyramids and TeO_3 trigonal pyramids by addition of both dopants. On the other hand, ultrasonic velocity was used to determine the elastic moduli of the glass such as bulk modulus, shear modulus, longitudinal modulus, Young's Modulus, microhardness and Poisson's ratio which showed decreasing and increasing trends with the increased concentration of MnO_2 and SrO respectively.

Introduction

Nowadays, glass is widely known as one of the most versatile materials on Earth which has been revealed in various forms for centuries. It can be defined as an amorphous solid that fuses together at its liquid state and undergoes rapid cooling to form rigid structures without having sufficient time to arrange to a crystalline structural order [1]. Glass is a non-crystalline solid that is often transparent and has a widespread practical, technological, and decorative usages such as window panes, tableware, and optoelectronics devices. The most familiar, and historically the oldest type of glass is "silicate glass" that is based on the chemical compound silica (silicon dioxide, or quartz), which is the primary constituent of sand. The properties of glass can be altered and changed when it combines with other materials. Thus, there are many research that have been done by doping various elements to the glass system in order to produce outstanding glass material.

Tellurite glass comes from a chemical compound named tellurium dioxide (TeO_2) as the main component of a glass system. From time to time, scientists have explored new glass systems by combining the tellurite glass system with other compositions such as rare earth oxide or transition metal. Tellurite based glasses are considered as the latest type of non-crystalline solid with many unique properties that can be utilized in the present modern industry. The various combinations in the chemical composition of tellurite glass system changes the internal structure of the glass and their overall properties. Therefore, it is important to investigate the changes that take place in the internal structure of the tellurite glass system since they are closely related to their properties. Tellurite glasses are considered as the best host materials for doping rare earth ions due to their good mechanical properties, good solubility, low cost, high thermal stability and ease of preparation [2].

Boron trioxide exhibits the appearance of white, glassy solid and has a molecular formula of B_2O_3 . Boron trioxide can be crystallized through extensive annealing process to alter its initial common amorphous form. One of its common applications is boron trioxide that can act as a glass former when it combines with the conditional glass former. Boron trioxide is considered to be the best choice of glass stabilizer due

to its hardness and good rare earth ion solubility. Borate matrix possesses BO_3 triangle and BO_4 tetrahedra that are able to form stable borate groups such as diborate, triborate and tetraborate. Such matrices indicate that borate has a strong B-O bonds hence granting its ability to form stable glasses.

Manganese dioxide is a brown or blackish solid with the molecular formula of MnO_2 . It is soluble in water. It is also normally used as a colorant as well as decolourizer in glass, white ware, enamels and pottery. It is also used in battery cathode mixes and electronics. MnO_2 is a promising material to be used in solid state lithium ion batteries for automobiles. In terms of strontium, it has been discovered by researchers to be a source that is biologically beneficial as it is being widely utilized for health purposes. The presence of strontium in calcium phosphate ceramic that is used for bone tissue repair has shown a positive feedback on the bone biology [3]. This strontium-contained bioactive bone cement is claimed to promote osteoblast attachment, mineralization in vitro and also bone growth.

Recently, tellurium dioxide is discovered to be equipped with many properties that can be explored for many applications. Tellurite oxide glass with altered structure is expected to form when it is combined with B_2O_3 , MnO_2 and SrO_2 . Therefore, the changes the properties of the original tellurite is expected to enhance the improvement of the glasses' properties based on previous researches and its potential application (high strength glass). In this research work, two different glass series had been studied in perspective of elastic, physical and structural properties. Despite of the unique properties possessed by borotellurite glass, none of the researches have tried to investigate the comparison between manganese oxide and strontium oxide on the mentioned properties. Hence, this work is proposed to be a new research and it can serve as a reference material in the future especially in the production of potential application of high strength glass.

Materials And Methods

Materials

Two glass series with the composition of $[(\text{TeO}_2)_{0.7} (\text{B}_2\text{O}_3)_{0.3}]_{1-x} [\text{MnO}_2]_x$ and $[(\text{TeO}_2)_{0.7} (\text{B}_2\text{O}_3)_{0.3}]_{1-x} [\text{SrO}]_x$ had been introduced using a TeO_2 , B_2O_3 , MnO_2 and SrO as the raw materials. The glass samples were produced strictly by following the procedure in order to get the best results. In this work, the glass samples were prepared by using the conventional melt quenching method. Melt quenching method was used due to its flexibility to produce glass. Different values of molar fraction were chosen where the dopant of manganese oxide and strontium dioxide, x were equivalent to 0.01, 0.02, 0.03, 0.04, and 0.05 molar fractions.

Method

Fabricating glass sample

Initially, before starting the actual procedure, the spatula, alumina crucible, mortar and pestle were washed and rinsed with acetone and water. Acetone was used as it is a solvent element for almost all

organic compounds while water is used to eliminate the compounds that cannot be dissolved by acetone. This step was to ensure that the apparatus used were thoroughly cleaned to avoid contamination in the samples.

The raw materials used in this research were tellurium (IV) oxide, TeO_2 (Aldrich 99.5%), boron trioxide, B_2O_3 (Alfa Aesar 99.99%), manganese (IV) oxide, MnO_2 (Alfa Aesar 99.99%) and strontium oxide, SrO (Alfa Aesar, 97.0%) in the form of solid powder. The weighing process was the initial step in order to produce the glass samples. An electronic weighing balance machine (with an accuracy of ± 0.0001 g) was used to weigh all the chemical powders. As the molar fraction changed with each series of the glass samples, the total weight of each composition also changed accordingly. The mixed chemical powders were then mixed thoroughly by mortar and pestle until it became homogenous before transferring into an alumina crucible.

The homogenous mixture then underwent preheating and melting process. In the glass preparation process, two furnaces were used. The alumina crucible that contained the homogenous mixture was placed in the first furnace for a preheating process at 400°C for one hour. The purpose of the preheating process was to remove excess water molecules which could affect the glass sample. After one hour, the alumina crucible was then moved to the melting furnace at 1000°C for two hours. The homogenous mixture in the alumina crucible was then melted for two hours in order to ensure the chemical powder mixture had blended with each other. At the same time, the stainless steel cylindrical shape split mould was inserted into the preheating furnace at 400°C for two hours. The mould was first polished to eliminate all the impurities on the surface of the mould that could cause contamination to the glass sample. The preheating of the mould was done in order to avoid thermal shock during the glass casting process which could cause cracks in the sample.

After two hours of melting process, the mould was taken out and the molten was casted into the preheated mould. The casting process should be done quickly to avoid crystallization and to ensure rapid cooling. After the casting process, the glass sample in the mould was transferred into the first furnace at 400°C for one hour for annealing process. Annealing process is intended to improve the mechanical strength and to remove the formation of air bubbles as well as to discourage the thermal stress from occurring. Then, the furnace was switched off and the glass sample was left to cool in the furnace overnight before being collected on the next day.

The surface of the sample was then polished by using silica carbide (SiC) abrasive sand paper with grade ranging from 800, 1000, 1200, 2400 and 4000 in ascending order. The polishing process was done until the surface of the glass sample became parallel, flat, and smooth. A vernier caliper was used to check and measure the thickness of the glass sample. The glass sample needed to be approximately 5.0 mm in thickness in order to be utilized for the elastic properties measurement. The remaining piece of the same glass sample was crushed and grounded into powder by using a plunger, mortar and pestle. Then, the processed sample was investigated for structural, physical and elastic analysis.

X-ray diffraction

In this work, X-Ray Diffraction (XRD) was employed in order to obtain structural information of the glass samples. Generally, XRD is a powerful tool for material characterization. It is commonly used to determine the structure of a glass and the orientation of single crystal grain. It can also be used to detect fragility in materials and to determine polymorphs as well. The data was collected for 2θ in the range of $20^\circ \leq \theta \leq 80^\circ$ [4].

Fourier Transform Infrared

Fourier transform infrared spectroscopy (FTIR) is a technique used to obtain infrared spectrum of absorption or emission of a solid, liquid or gas. FTIR spectrometer is able to obtain high-spectral-resolution data over a wide spectral range. The term Fourier Transform Infrared spectroscopy was used due to its strong correlation to its mathematical method requiring a reverse signal to attain sample information. The purpose of FTIR being used in this research is to identify the chemical bond that exists in the glass samples. This method works by exposing infrared radiation onto the glass samples. Some of the radiation was absorbed by the samples, while the rest were transmitted. The absorption of different range of wavenumber indicates different types of chemical bond that are present in the glass samples.

Density And Molar Volume

Physical analysis done on the glass samples includes density and molar volume parameters. Density is defined as;

Density = mass / volume (1)

Besides, it can also be identified as a measurement of compactness of matter within a certain substance. The determination of density utilizes Archimedes' principle where it states that the buoyant force on a submerged object is equivalent to the weight of the fluid displaced by the object. If the glass sample float, it means that the weight of water displaced is equal to the weight of the glass sample. An electronic densimeter MD-300S with accuracy up to $\pm 0.01 \text{ g/cm}^3$ was used to measure the density of the glass sample. The measurement was done in a room temperature with distilled water as the immersion liquid. Distilled water is suitable to be used compared to acetone because acetone vaporizes easily at room temperature. The instrument was first calibrated to avoid zero error before taking the actual density of the glass sample. The glass sample was then placed slowly in distilled water and the mass of the immersed glass sample was measured. The density of the glass could be calculated by using the following formula:

$$\rho_{sample} = \frac{W_{air}}{W_{water}} \times \rho_{water}$$

where $\rho_{water} = 1 \text{ g/cm}^3$, W_{air} is the weight of the sample in the air and W_{water} is the weight of the sample in distilled water. The molar volume of the glass sample could then be calculated from the formula, $V_m = \frac{M}{\rho}$, where V_m is the molar volume in cm^3/mol , M is the total molecular weight of the glass sample in g/mol and ρ_{sample} is the density of the glass sample in g/cm^3 .

Ultrasonic velocity

Ultrasonic method makes use of the velocity of ultrasonic waves that relies on the elastic properties of the propagation medium. As compared with the conventional indentation and tensile test, the ultrasonic test provides better repeatability and yields more precise results. In this work, ultrasonic through transmission method had been performed as the base approach in order to obtain the experimental elastic properties of the glass samples. This method is commonly used in various fields such as composite medicine and biomaterials [5]. The propagation velocity of the ultrasonic wave such as shear and longitudinal waves relies on the properties of the materials. However, the propagation velocity of the ultrasonic wave of a given material is independent from its frequency and dimension. For isotropic and homogenous glassy material, the one dimensional wave can be revealed as either shear node compressional wave or transverse wave and longitudinal node. Throughout this study, MATEC 8000 system was used to carry out the ultrasonic measurement. Ultrasonic instrument was operated in pulse-echo mode, using the same transducer for transmitting and receiving ultrasonic wave. The principle behind the operation of obtaining the velocities was based on the pulse echo overlap technique via the Digital Signal Processing (DSP). There were two types of transducers used for obtaining the shear and longitudinal velocities in this work. The X-cut transducer was used to generate longitudinal wave while the Y-cut transducer was used to generate transverse wave. A couplant was used to ensure a good contact between the glass sample and the transducer so that the loss of acoustic energy could be minimized due to unwanted reflection [6]. The pulse echo pattern displayed only two consecutive echoes on the oscilloscope screen which were chosen to obtain the velocities. The measured longitudinal and shear velocities of the sample were then used to evaluate the elastic moduli of the glass samples.

In order to obtain the information regarding the elastic properties of the material, elastic moduli were a vital approach used in this project.

The elastic moduli of a matter are investigated by the vibration, interatomic forces, and the structure of the material [7].

Elastic properties

The technique used for investigating the elastic moduli of a solid material can be divided into two methods, static and dynamic. The static method applies the calculation of stress-strain curve in the elastic deformation limit where the elastic moduli are determined from the gradient of stress-strain. However, this method is difficult to apply to material like glass because of its fragility. This is where the dynamic method plays a vital role as it offers relatively high accuracy results. In addition, dynamic

method is widely used in determining the elastic properties and elastic moduli of glasses as well as glass-forming liquid.

Results And Discussion

X-ray diffraction (XRD)

The X-ray diffraction (XRD) analysis was used to determine whether the material was in amorphous or crystalline state. The X-ray diffraction patterns of the prepared borotellurite glasses doped with manganese dioxide and strontium oxide were recorded. The following figures showed the XRD diffraction patterns of the two glass series.

Both Figures 1 and 2 showed broad hump patterns in the XRD spectra. Broad humps for both glass series indicated the presence of long range structural disorder [4]. Meanwhile, Rosmawati et al. (2008) [8] stated that the absence of sharp and strongly diffracted beams in the glass X-ray diffraction pattern indicated that there were no well-defined planes in the structure. Hence, the broad hump pattern in the XRD analysis confirmed that the prepared glass samples were in amorphous state.

Fourier Transform Infrared (FTIR)

FTIR spectroscopy measurement was a technique that was mainly used to obtain and explain the internal structural unit and the fundamental groups in the studied glass systems. The infrared spectra of absorption and transmission in the glass samples explained the characteristic of every molecule. The FTIR spectra of the glass samples were recorded in the range of $280-1680\text{ cm}^{-1}$ and shown in Figure 3 and 4. The observed broad bands could be associated with a combination of higher degeneracy of vibrational states, thermal broadening of the lattice dispersion, mechanical scattering of the powdered samples and the corresponding band assignments [9].

The FTIR spectra had several peaks specifying its local structure. For every structure, specific frequencies had been assigned. Table 1 showed the peak positions and its assignments from the FTIR result.

Table 1: Assignment of infrared transmission bands of the prepared glass samples with different concentration of manganese dioxide and strontium oxide.

No	0.01	0.02	0.03	0.04	0.05	Assignment
1	654.21	653.81	656.28	656.11	655.17	TeO ₄ group existed in all tellurite containing glass ranging from 600-665 cm ⁻¹ [10].
2	1216.85	1215.45	1216.73	1218.56	1217.28	Trigonal B-O bond stretching vibration of BO ₃ units from boroxyl groups ranging from 1200-1500 cm ⁻¹ [10].
3	1350.98	1364.74	1346.40	1341.81	1355.57	The stretching vibration of the B-O of trigonal (BO ₃) units were assigned at 1350 cm ⁻¹ [11].

Tellurite oxide consists of two types of structural configuration units which are trigonal bipyramid TeO₄ and trigonal pyramid, TeO₃. Pure TeO₂ was characterized around 640 cm⁻¹. Meanwhile, the absorption band at 600 – 700 cm⁻¹ was assigned as the stretching vibration of Te-O bonds. The stretching vibration of TeO₃ posed higher frequency (665-700 cm⁻¹) rather than TeO₄ stretching vibration (600-665 cm⁻¹) [12]. In this work, TeO₄ group was found to exist in the range of 654 – 656 cm⁻¹ which was in the normal range of TeO₄. The absorption band of pure borate glass, B₂O₃ was centered at 806 cm⁻¹, indicating characteristics of boroxyl ring [9]. As the absorption spectra indicated the absence of boroxyl ring, BO₃ and BO₄ appeared as the substitution to the boroxyl ring [10]. In this work, the absorption band positioned at 1215 – 1218 cm⁻¹ was assigned to the trigonal B-O bond stretching vibration of BO₃ units from boroxyl groups. The absorption band at 1350 – 1364 cm⁻¹ was assigned to the stretching vibration of the B-O of trigonal (BO₃) units [13]. Meanwhile, the manganese oxide and strontium dioxide could not be detected in the FTIR spectra due to the small amount of dopants' concentration.

Physical analysis

Density and molar volume

The calculated density and molar volume of the prepared glass samples were recorded in Table 2.

Table 2: Density and molar volume of borotellurite glass doped with manganese oxide and strontium dioxide

Molar fraction, x	Density Mn (g/cm ³)	Molar volume Mn (cm ³ /mol)	Density Sr (g/cm ³)	Molar volume Sr (cm ³ /mol)
0.01	3.505	37.700	2.8280	46.7877
0.02	3.323	39.649	3.2976	40.0350
0.03	3.113	42.149	3.6462	36.1295
0.04	3.108	42.069	3.7501	35.0512
0.05	3.066	42.503	3.8053	34.4663

From the table above, it could be observed that as the concentration of manganese dioxide increased, the density of the prepared glass sample decreased. The increase of manganese cation concentration made the structure of the glass to become more spaced out, producing higher numbers of non-bridging oxygen (NBO) [15]. The introduction of manganese dioxide ruptured some of the BO_4 and TeO_4 bonds transforming them into BO_3 and TeO_3 which created more NBO. The decrease in density of the glass samples was also due to the addition and substitution of lighter and manganese dioxide as compared to tellurite. The atomic mass of manganese dioxide is 86.9368 g/mol while the atomic mass of borate is 69.6182 g/mol which are both lighter compared to tellurium (127.60 g/mol). Hence, this caused the density to decrease as the molar fraction increased. This result also agreed with Doweider and Saddek (2009) [16] which stated that density will change if there was replacement of atom in the glass network.

According to Krogh Moe. (1962) [17], the conversion from the trigonal boron atom (BO_3) into four-fold (BO_4) coordinated boron atom could occur upon modification by an alkali oxide through the creation of bridging oxygen network between each BO_4 negatively charged structural group and four oxygen. This phenomenon led to the changes in composition that were proven by the density result which reflected the underlying atomic arrangements in a quantitative manner. The increment in the density was attributed by the factors of conversion BO_3 triangles into BO_4 tetrahedral which was due to the insertion of the higher atomic weight of strontium (87.62 amu). In addition, the increment of the oxygen-boron ratio could also influence the increment of density as the concentration of SrO increased [18]. The smaller ionic radius of strontium ion, Sr^{2+} ($118 \cdot 10^{-12}$ m) compared to tellurium ion, Te^{4+} ($221 \cdot 10^{-12}$ m) forces the strontium ions to fit into the interstitial spaces of the glass network in order to form the BO_4 groups which then led to the increment of density, resulting in improvement of the glass system compactness.

Molar volume was inversely proportional to the density of the glass sample. This explains that as the density decreased, the molar volume increased. As displayed in Figure 6, the increment of molar volume was directly proportional to the molar fraction of manganese dioxide in the glass sample. Based on Azianty et al., (2012) [19], the increment of NBO in the glass network had been proposed as the reason behind the increment in molar volume values. The experimental result adhered to the theoretical result which stated that density was inversely proportional to molar volume. The increase in the formation of NBO in the glass structure encouraged the rise in molar volume due to the production of more interatomic

space between the molecules. Therefore, the glass structure became less dense. Besides that, the increment of molar volume may be attributed by the increase in bond length and inter atomic spacing between the atoms [20]. The introduction of manganese dioxide ion affected the bond length between the atoms. This was because manganese dioxide had $\sim 1.900 \text{ \AA}$ bond length compared to tellurium that had 2.684 \AA bond length. This imbalance in bond length between manganese and tellurium also caused more interspatial space to be created in the glass structure thus, causing an increase in the molar volume.

The calculated molar volume of the prepared glass samples was also recorded in Table 4.2. Based on Figure 8, the molar volume graph showed a decrement behavior from the density graph as the molar fraction of strontium oxide increased. This might be due to the fact that there was an incorporation of strontium ion of radii 1.12 \AA to replace the tellurium ion of radius 0.97 \AA which altered the stretching of the glass network. The current trend of molar volume was also similar to the result obtained by Norihan et al. (2018) [21].

Elastic properties

Elastic properties provides information about the internal arrangement of constituent elements and the mechanical strength of the glass [22,23,24]. In this work, the elastic constants and the other physical parameters were evaluated from the experimental measurements obtained by using ultrasonic velocities in the glass system. From this technique, shear and longitudinal velocities could be obtained as they were vital parameters in order to identify the other elastic parameters. Glasses were considered as elastic substance which could be characterized by using ultrasonic non-destructive technique or pulse-echo technique. According to Halimah et al. (2010) [14], glasses were isotropic and had only two independent elastic constants which were longitudinal and shear elastic moduli. Both of those parameters were obtained from the ultrasonic velocities and density of the glass.

Table 3: Longitudinal and shear velocities of Mn and Sr-doped borotellurite glass

Molar fraction	Mn-doped glass		Sr-doped glass	
	v_L (m/s)	v_S (m/s)	v_L (m/s)	v_S (m/s)
0.01	3790	2200	8334	4401
0.02	3760	2190	7427	4317
0.03	3820	2230	7582	4344
0.04	3860	2240	7227	4185
0.05	3900	2250	7849	4482

As observed in manganese oxide glass, for longitudinal velocity, the value dropped at $x=0.01$ until $x=0.02$ from 3790 m/s to 3760 m/s , then it increased gradually from $x=0.03$ molar fraction onward. The same trend followed in shear velocity as it dropped at $x=0.01$ until $x=0.02$ from 2200 m/s to 2190 m/s , then the

value went up from 2230 m/s to 2250 m/s ahead. For strontium glass, it could be seen that both ultrasonic velocities, v_L and v_S showed the same decreasing trend for molar fraction of $x=0.01$ to $x=0.02$. The v_L values decreased from 8334 m/s to 7427 m/s while v_S values decreased from 4406 m/s to 4317 m/s respectively with the addition of SrO. However, v_L and v_S increased from 7427 m/s at $x=0.02$ to 7582 m/s at $x=0.03$ and 4317 m/s at $x=0.02$ to 4344 m/s at $x=0.03$ respectively. Meanwhile, for the molar fraction of $x=0.04$, a decreasing trend was observed for both ultrasonic velocities. The v_L values dropped from 7582 m/s to 7227 m/s and v_S values dropped from 4344 m/s to 4185 m/s before both parameters went up to 7849 m/s and 4482 m/s respectively.

The ultrasonic velocities were strongly related to the density parameter. Both of the parameters were directly proportional to each other. The decrement of velocities at a certain concentration could be associated with the open structure of the glass samples, producing numbers of non-bridging oxygen within the glass system. The bridging oxygen (BO) was said to turn to NBO in the glass samples. This conversion made the glass samples became less rigid. The reduction in ultrasonic velocities could be attributed by the inferior packing density which was possibly caused by the increase in molar volume [25]. Besides that, this declining trend could be better explained by the action of manganese oxide and strontium oxide that acted as a modifier to produce cleavages in the glass network [26]. This was also agreed by a study from Halimah et al. (2010) [14]; which stated that the decreasing trend could be associated with the splitting of Te-O-Te and O-B-O bonds due to the conversion of non-bridging oxygen (NBO) from bridging oxygen (BO).

Some parts involving an increase in ultrasonic velocity values could also be observed. According to Hasnimulyati et al. (2016) [27], the rising trend of these parameters indicated the strengthening of the glass network and the increase in the rigidity of the glass samples. The transformation of BO_3 triangular boron into BO_4 tetrahedral boron coordination and the formation of TeO_4 trigonal bipyramid were the factors that described the increase in the glass rigidity. Besides, the increase of packing density in the glass network could also enhance the increment of both longitudinal and shear velocities [28].

Table 4: Elastic moduli of Mn and Sr-doped borotellurite glasses

Molar fraction, x	Mn-doped glass				Sr-doped glass			
	L (GPa)	G (GPa)	K (GPa)	Y (GPa)	L (GPa)	G (GPa)	K (GPa)	Y (GPa)
0.01	50.40	16.77	28.04	41.95	196.40	54.89	143.38	123.21
0.02	46.95	16.09	25.50	39.87	181.91	61.47	153.04	99.95
0.03	45.43	15.42	24.87	38.34	209.58	68.80	172.78	117.85
0.04	45.26	15.35	25.39	38.95	195.86	65.68	163.91	108.28
0.05	45.14	15.49	25.89	38.74	234.43	76.46	192.37	132.48

The trends were discussed according to their respective dopants which were manganese oxide and strontium oxide. The shear modulus and longitudinal modulus decreased as the molar fraction of MnO_2 increased. Generally, both moduli depended on the trend of density as they were directly proportional to each other. The decrement of both moduli could be associated with the increment in number of NBO, which intruded the glass network and discouraged the rigidity and connectivity of the glass samples. The manganese ion filled the interstitial position and produced Mn-O bonds which then decreased its rigidity as it produced more free spaces within the glass structure.

For strontium oxide, the decrement in the elastic moduli was significant to the increment in number of non-bridging oxygen (NBO) group with more open structure as the network modifier (strontium ions) broke the network structure, similar to the ability of manganese as stated before. However, when molar fraction of strontium oxide was $x = 0.01$, an opposite trend for both longitudinal and shear moduli was observed. Longitudinal modulus (L) showed high decrement from 196.40 GPa to 181.91 GPa and shear modulus (G) showed high increment from 54.89 GPa to 61.47 GPa. These differences might be caused by the drastic structural modification against the respective forces imposed on the shear and longitudinal directions. The same reason also contribute to the reduction of bulk modulus (K), from 123.21 GPa to 99.95 GPa. Nazrin et al. (2018) proposed that the reduction in both bulk and Young's moduli encouraged the number of formation in non-bridging oxygen (NBO) group that will eventually encourage more open structure. The declination in the rigidity of the glasses had been proved by the FTIR result, displayed by the shifting of the TeO_4 ($\sim 605.91 \text{ cm}^{-1}$) peaks to higher wavenumber. This indicated the structural distortion due to the transformation of TeO_4 trigonal bipyramid to TeO_3 trigonal pyramid structures which contributed to the increase in non-bridging oxygen (NBO) [19].

Meantime, the increment of bulk modulus from 0.02 to 0.05 molar fraction of Mn suggested the increment in bridging oxygen (BO) [19]. Specifically, for Young's modulus, the fluctuating trend could be associated with the competition of NBO and BO. This indirectly agreed that the increment and decrement trends promoted the presence of BO and NBO. According to Pavai and Indhira (2015) [29], the inclination in the elastic constant was also attributed by the large packing density that enhanced the rigidity of the

glass network and by the increment of bridging oxygen (BO) ions in the glass network that was more abundant as indicated by the relative intensity of TeO_4 trigonal bipyramid.

Apart from the creation of non-crystalline phase induced by the addition of the strontium oxide, the oxygen from the dopant could break the local symmetry of tellurite bond and fill into interstitial position, therefore producing a strong covalent bond that increased the rigidity of the glass network [12]. It could be clearly seen that there was a huge difference of values where longitudinal modulus (L) ranged around 200 GPa while shear modulus ranged around 70 GPa. According to Pavai and Indhira (2015) [29], the effect of volume in glass could be associated with the presence of compression and expansion, provided the major impact was on longitudinal strain rather than on the shear strain. According to Afifi and Marzouk (2003) [30], the high rigidity of the glass might also be attributed by the role of strontium ions that are encompassed within the interstices of the glass. Therefore, the rigidity of the glasses increased.

Table 5: Poisson's ratio, σ of Mn and Sr-doped borotellurite glasses

Molar fraction, x	Mn-doped glass	Sr-doped glass
0.01	0.251	0.3060
0.02	0.239	0.2448
0.03	0.243	0.2556
0.04	0.244	0.2477
0.05	0.251	0.2580

For the trend of Poisson's ratio, most of the values ranged from 0.2 to 0.3. Poisson's ratio was defined as the ratio of lateral to longitudinal strain when tensile forces were exerted [12]. Tensile strain created was not affected by the cross link but the lateral strain will be affected by the existence of cross link density. This was because, a high cross-link generated a strong covalent force to resist lateral contraction and thus, resulting in a decrease of Poisson's ratio value. The addition of manganese dioxide into the glass interstices led to more ions to open up within the glass network. Hence, the glass structure will be weak and loosely packed, causing the splitting of TeO_2 and B_2O_3 from bridging oxygen (BO) to non-bridging oxygen (NBO). This eventually made the glass less rigid. A decrease in rigidity of glass caused the decrease in ultrasonic velocities and and thus, an increase in the Poisson's ratio [19]. The glass was also considered as high cross link density due to its low range of order from 0.2 to 0.3.

In Figure 15, the decrement of Poisson's ratio values was observed from 0.3060 to 0.2448 at $x = 0.01$ molar fraction and from 0.2556 to 0.2477 at $x = 0.03$ molar fraction of SrO. This condition might be referred to the increase in the covalent cross-linking as a result of the transformation of B-O-B into B-O-Sr bonds. Meanwhile, the increment of Poisson's ratio values from 0.2448 to 0.2556 at $x = 0.02$ molar fraction and from 0.2477 to 0.2580 at $x = 0.04$ molar fraction was mainly due to the change in the type of

bonding from covalent bond to ionic bond as the glass network started to change from the continuous borate structure to the strontia structure. In addition, a similar trend in the respective regions had been reported by Bridge and Higazy (1986) [31], in the study of ZnO-P₂O₅ and CoO-P₂O₅ glasses. According to Gaafar et al. (2009) [32], the decreasing trend of Poisson's ratio in the first region was associated with the increase in cross-link density, while the increase in the second region was associated with the fact that there was a presence of Zn²⁺ and Co²⁺ ions in octahedral coordination. The Poisson's ratio was directionally weak and produced a low ratio of bending force constant with respect to the stretching force constant. This was similar in the present study referring to the declining trend of Poisson's ratio in the first region that was due to the increase in cross-link density. In the second region, the presence of SrO²⁻ ions produced a low ratio of bending force constant that was fully linked to the stretching force constant [33].

Conclusion

In this research the melt quenching technique method was used to synthesize two series of borotellurite glass systems doped with manganese oxide and strontium oxide with chemical compositions of [(TeO₂)_{0.7} (B₂O₃)_{0.3}]_{1-x} [MnO₂]_x and [(TeO₂)_{0.7} (B₂O₃)_{0.3}]_{1-x} [SrO]_x with different molar fractions x = 0.01, 0.02, 0.03, 0.04, and 0.05. All glass samples were amorphous in nature since there was no sharp peak observed in the X-Ray diffraction (XRD) result. The Fourier Transform Infrared spectroscopy (FTIR) indicated the existence of TeO₄ and BO₃ units' stretching vibration in the glass sample. The density of the glass sample decreased as the molar fraction of manganese oxide increased but decreased when the molar fraction of strontium oxide increased. For manganese dopant, this was due to the substitution of lighter atomic mass of manganese as compared to tellurium. In contrast, the inclination in the density value was caused by the existence of the excess oxygen due to the presence of TeO₄ functional groups as well as by the addition and substitution of heavier strontium atomic mass (87.62 g/mol) as compared to the other present atoms found in the glass sample. The molar volume of the glass sample showed an opposite trend with density. The parameters of density and molar volume were strongly related to the connectivity within the glass network.

The pulse echo overlap method at MHz was used to determine the elastic properties of glass sample by evaluating the shear and longitudinal velocities to which the results showed both increasing and decreasing trends as expected. The creation of NBO made the glass structure became more open and less rigid and it was also influenced by the values of the related moduli. The decreased value of related moduli was due to the creation of NBO which was considered to distract the glass network and decrease the rigidity and the connectivity of the glass network. Elastic properties might be affected by the structural changes that corresponded to the variation of the molar fraction. In this research, the behavior of elastic properties with different molar fraction was also related to the density and molar volume.

Based on high strength glass application, the values of density, molar volume and Poisson's ratio for both dopants are comparable. Nevertheless, the values of elastic parameters for strontium oxide displayed higher values than manganese oxide. The strontium oxide was believed to improve the strength of the

glass as it has the ability to increase density and compactness. The ability of strontium to increase the density and other elastic parameters was influenced by the strontium's atomic weight that is slightly higher than manganese's atomic weight.

In the future, the elastic properties of borotellurite glasses doped with both manganese and strontium oxides can be investigated under various thicknesses of the glass sample to observe the effect of thickness to the elastic properties. The frequency of the ultrasonic measurement can also be varied to see its effect on the elastic properties. This project result may be used to support further elastic behavior of the glass system in the future. The borotellurite glasses doped with manganese dioxide and strontium oxide can also be studied even more by investigating other properties of the materials such as thermal, dielectric, electrical and optical properties.

Declarations

Declaration of Competing Interest

The authors declare that they have no known competing interests that could have influenced the research presented in this article.

Acknowledgement

The authors extend their appreciation to the Deanship of Scientific Research at King Khalid University, Saudi Arabia for funding this work through Research Groups Program under grant number R.G.P/1/93/42.

References

1. A. Pradel, F. Henn, J.L. Souquet, M. Ribes, Use of a thermodynamic model to interpret Li⁺ ionic conduction in oxide and sulphide binary glasses. *Philosophical magazine B* **60**(6), 741–751 (1989)
2. P. Giridhar, S. Sailaja, M.B. Reddy, K.V. Raju, C.N. Raju, B.S. Reddy, Spectroscopic studies of RE³⁺ (RE = Eu, Tb, Sm & Dy): lithium lead boro tellurite glasses. *Ferroelectr. Lett.* **38**(1–3), 1–10 (2011)
3. A.A. Gorustovich, J.A. Roether, A.R. Boccaccini, Effect of bioactive glasses on angiogenesis: a review of in vitro and in vivo evidences. *Tissue Engineering Part B: Reviews* **16**(2), 199–207 (2010)
4. M. Hamezan, H.A.A. Sidek, A.W. Zaidan, K. Kaida, A.T. Zainal, Elastic constants and thermal properties of lead-bismuth borate glasses. *Journal of Applied Sciences* **6**(4), 943–949 (2006)
5. E.E. Franco, J.M. Meza, F. Buiochi, Measurement of elastic properties of materials by the ultrasonic through-transmission technique. *Dyna* **78**(168), 58–64 (2011)
6. S.A. Aziz, *Wonders of Glass: Synthesis, Elasticity and Application* (Penerbit Universiti Putra Malaysia, 2011)
7. W.H. Wang, The elastic properties, elastic models and elastic perspectives of metallic glasses. *Prog. Mater Sci.* **57**(3), 487–656 (2012)

8. S. Rosmawati, H.A.A. Sidek, A.T. Zainal, M. Zobir, H, Effect of zinc on the physical properties of tellurite glass. *Journal of Applied Sciences* **8**(10), 1956–1961 (2008)
9. S.S. Hajer, M.K. Halimah, Z. Azmi, M.N. Azlan (2014). OPTICAL PROPERTIES OF ZINC-BOROTELLURITE DOPED SAMARIUM. *Chalcogenide Letters*, *11*(11)
10. A. Muhammad Noorazlan, M. Kamari, H. Zulkefly, S. S., & D.W. Mohamad (2013). Effect of erbium nanoparticles on optical properties of zinc borotellurite glass system. *Journal of Nanomaterials*, *2013*
11. S. Rada, P. Pascuta, M. Rada, E. Culea, Effects of samarium (III) oxide content on structural investigations of the samarium–vanadate–tellurate glasses and glass ceramics. *J. Non-cryst. Solids* **357**(19–20), 3405–3409 (2011)
12. S.N. Nazrin, M.K. Halimah, F.D. Muhammad, J.S. Yip, L. Hasnimulyati, M.F. Faznny, I. Zaitizila, The effect of erbium oxide in physical and structural properties of zinc tellurite glass system. *J. Non-Cryst. Solids* **490**, 35–43 (2018)
13. M.A. Hazlin, M.K. Halimah, F.D. Muhammad, M.F. Faznny, Optical properties of zinc borotellurite glass doped with trivalent dysprosium ion. *Physica B* **510**, 38–42 (2017)
14. M.K. Halimah, W.M. Daud, H.A.A. Sidek, A.W. Zaidan, A.S. Zainal, Optical properties of ternary tellurite glasses. *Mater. Sci. Pol* **28**(1), 173–180 (2010)
15. S.P.H.S. Hashim, H.A.A. Sidek, M.K. Halimah, K.A. Matori, W.M.D.W. Yusof, M.H.M. Zaid, The effect of remelting on the physical properties of borotellurite glass doped with manganese. *Int. J. Mol. Sci.* **14**(1), 1022–1030 (2013)
16. H. Doweidar, Y.B. Saddeek, FTIR and ultrasonic investigations on modified bismuth borate glasses. *J. Non-Cryst. Solids* **355**(6), 348–354 (2009)
17. J. Krogh-Moe, The crystal structure of lithium diborate, $\text{Li}_2\text{O} \cdot 2\text{B}_2\text{O}_3$. *Acta Crystallogr. A* **15**(3), 190–193 (1962)
18. H.K. Obayes, R. Hussin, H. Wagiran, M.A. Saeed, Strontium ion concentration effects on structural and spectral properties of $\text{Li}_4\text{Sr}(\text{BO}_3)_3$ glass. *J. Non-Cryst. Solids* **427**, 83–90 (2015)
19. S. Azianty, A.K. Yahya, M.K. Halimah, Effects of Fe_2O_3 replacement of ZnO on elastic and structural properties of $80\text{TeO}_2-(20-x)\text{ZnO}-x\text{Fe}_2\text{O}_3$ tellurite glass system. *J. Non-cryst. Solids* **358**(12–13), 1562–1568 (2012)
20. Halimah, M. K., Sidek, H. A. A., Daud, W. M., Zainul, H., Talib, Z. A., Zaidan, A.W., ... Mansor, H. (2005). Ultrasonic study and physical properties of borotellurite glasses. *Am. J. Appl. Sci.* *2*(11), 1541-6
21. Yahya, N., Kasim, A., Hashim, A., Rafien, S. N., Razali, W. A. W., Senawi, S. A.,... Abdullah, M. (2018). Effect of silver on the physical and structural properties of lead neodymium borotellurite glass system. *Malaysian Journal of Analytical Sciences*, *22*(2), 296–302
22. M.K. Halimah, W.M. Daud, H.A.A. Sidek, A.S. Zainal, A.H. Zainul, H. Jumiah, Structural analysis of borotellurite glass. *Am. J. Appl. Sci* **5**, 323–327 (2007)

23. Y.B. Saddeek, H.A. Afifi, N.S. Abd El-Aal, Interpretation of mechanical properties and structure of $\text{TeO}_2\text{-Li}_2\text{O-B}_2\text{O}_3$ glasses. *Physica B* **398**(1), 1–7 (2007)
24. N.S. Sabri, A.K. Yahya, R. Abd-Shukor, M.K. Talari, Anomalous elastic behaviour of $x\text{SrO-}10\text{PbO-(90-x)}\text{B}_2\text{O}_3$ glass system. *J. Non-Cryst. Solids* **444**, 55–63 (2016)
25. Y.B. Saddeek, Elastic properties of Gd^{3+} -doped tellurovanadate glasses using pulse-echo technique. *Mater. Chem. Phys.* **91**(1), 146–153 (2005)
26. H. Gebavi, D. Milanese, G. Liao, Q. Chen, M. Ferraris, M. Ivanda, S. Taccheo, Spectroscopic investigation and optical characterization of novel highly thulium doped tellurite glasses. *J. Non-cryst. Solids* **355**(9), 548–555 (2009)
27. L. Hasnimulyati, M.K. Halimah, Z. Azmi, A.H. Shaari, M. Ishak (2016). Elastic properties of thulium doped zinc borotellurite glass. In *Materials Science Forum* (Vol. 863, pp. 70–74). Trans Tech Publications Ltd
28. C. Eevon, M.K. Halimah, Z. Azmi, C. Azurahaman, Elastic properties of $\text{TeO}_2\text{-B}_2\text{O}_3\text{-ZnO-Gd}_2\text{O}_3$ glasses using non-destructive ultrasonic technique. *Chalcogenide Letters* **13**(6), 281–289 (2016)
29. R.E. Pavai, M. Indhira (2015). Study of elastic properties of potassium borate glasses doped with barium oxide. *International Journal of Innovative Research in Science, Engineering and Technology*, 7244–7252
30. H. Afifi, S. Marzouk, Ultrasonic velocity and elastic moduli of heavy metal tellurite glasses. *Mater. Chem. Phys.* **80**(2), 517–523 (2003)
31. B. Bridge, A.A. Higazy, Acoustic and optical Debye temperatures of the vitreous system $\text{CoO-Co}_2\text{O}_3\text{-P}_2\text{O}_5$. *J. Mater. Sci.* **21**(7), 2385–2390 (1986)
32. M.S. Gaafar, Y.B. Saddeek, L. Abd El-Latif, Ultrasonic studies on alkali borate tungstate glasses. *J. Phys. Chem. Solids* **70**(1), 173–179 (2009)
33. N. Baizura, A.K. Yahya, Effects of Nb_2O_5 Replacement by Er_2O_3 on elastic and structural properties of $75\text{TeO}_2\text{-(10-x)}\text{Nb}_2\text{O}_5\text{-}15\text{ZnO-(x)}\text{Er}_2\text{O}_3$ glass. *J. Non-cryst. Solids* **357**(15), 2810–2815 (2011)

Figures

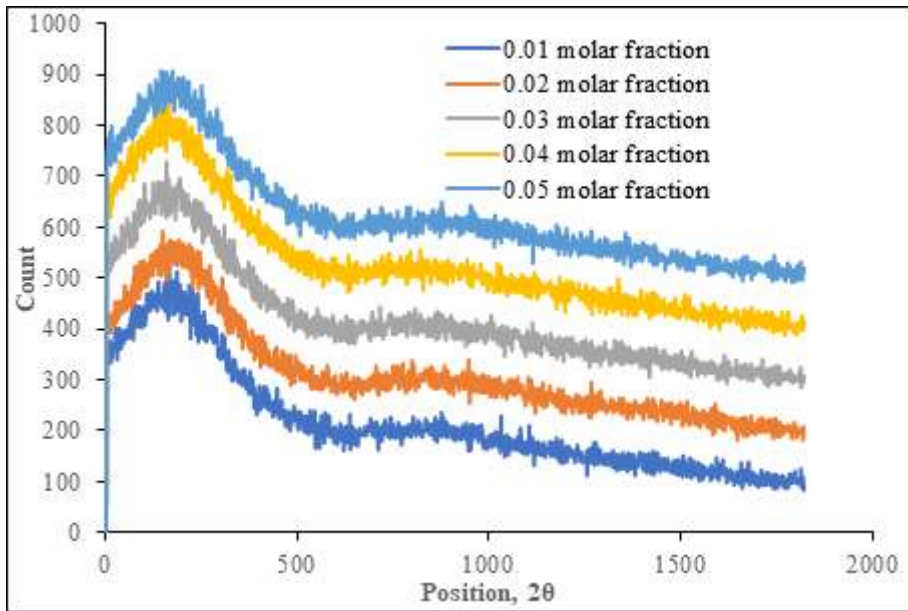


Figure 1

XRD diffraction pattern of prepared glass samples with different concentration of manganese dioxide

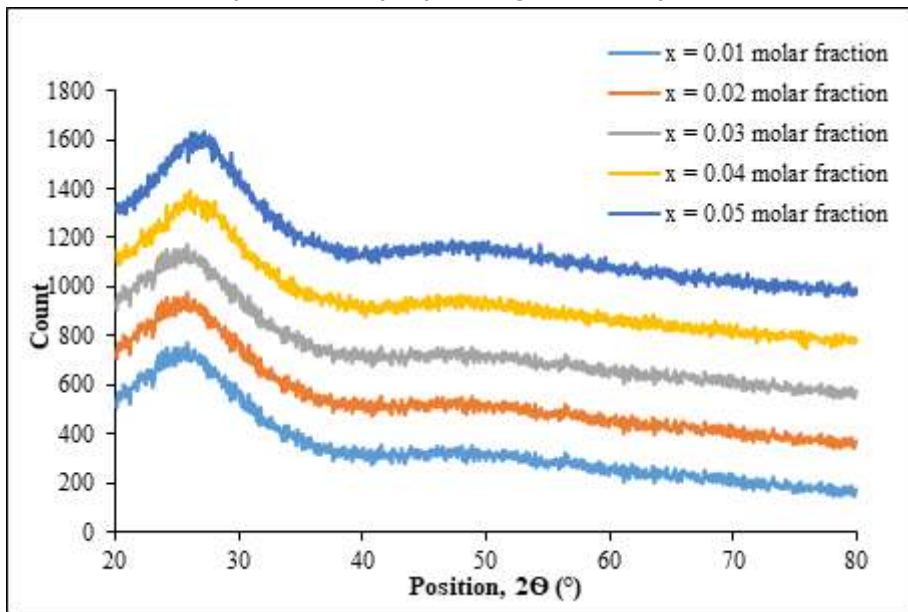


Figure 2

XRD diffraction pattern of prepared glass samples with different concentration of strontium dioxide

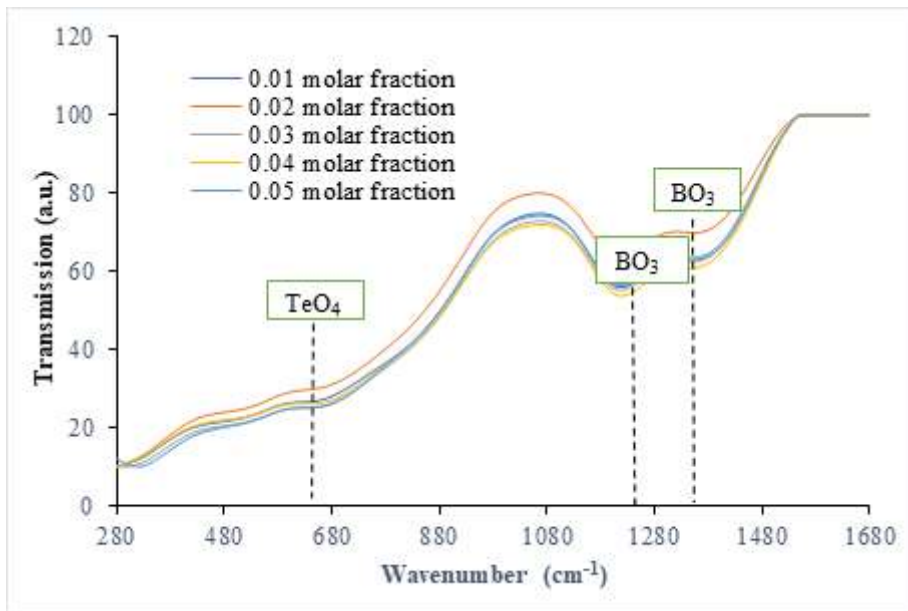


Figure 3

FTIR spectra of prepared glass samples with different concentration of manganese dioxide.

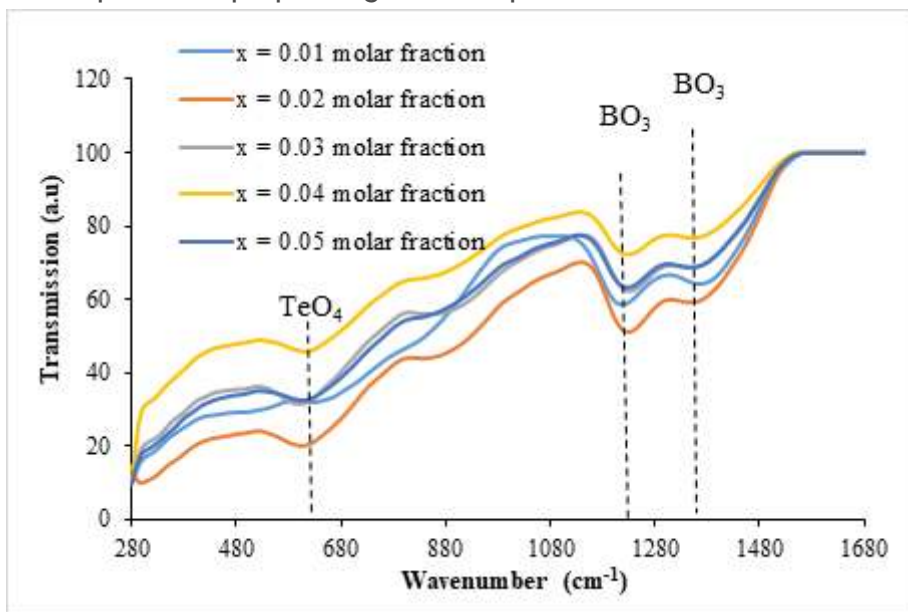


Figure 4

FTIR spectra of prepared glass samples with different concentration of strontium dioxide.

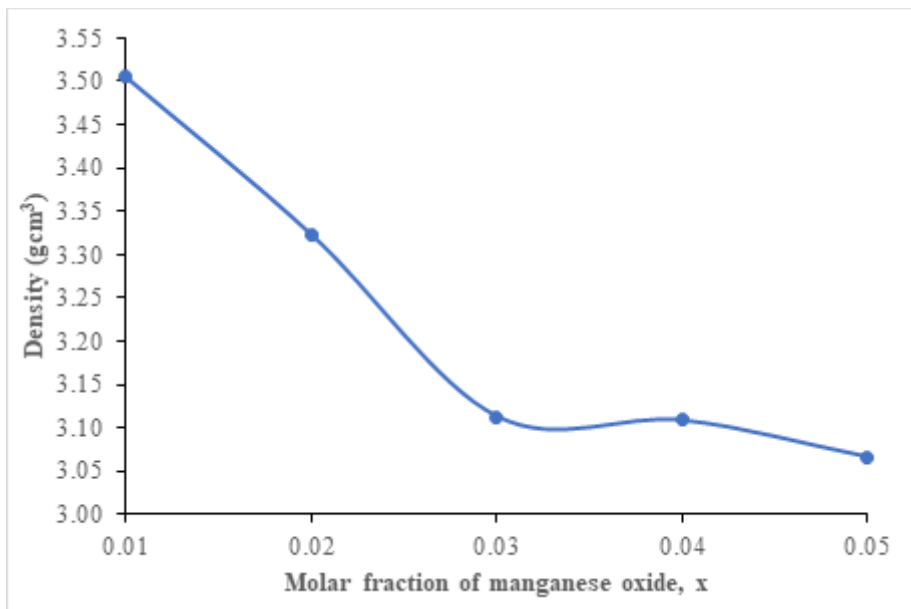


Figure 5

Density of borotellurite glass doped with manganese oxide

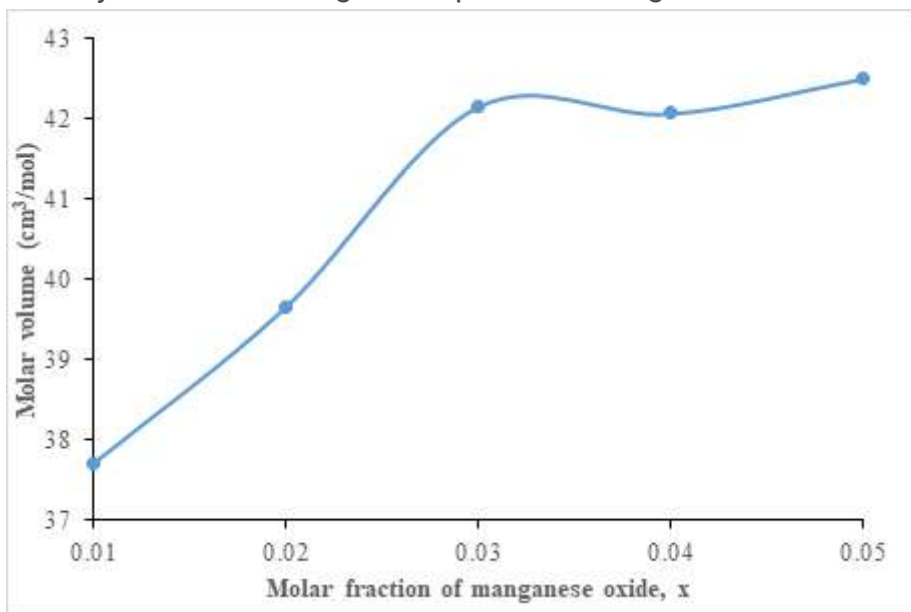


Figure 6

Molar volume of borotellurite glass doped with manganese oxide

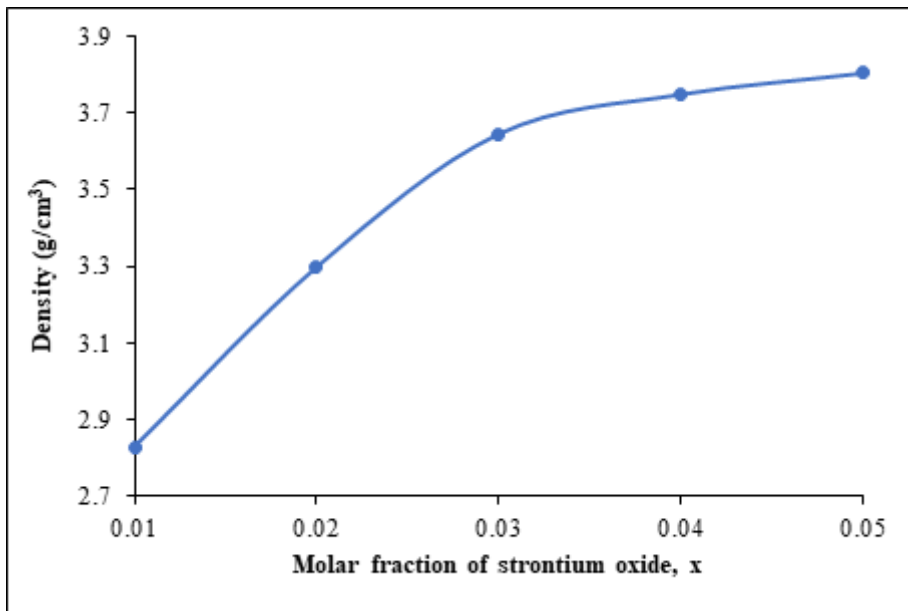


Figure 7

Density of borotellurite glass doped with strontium oxide.

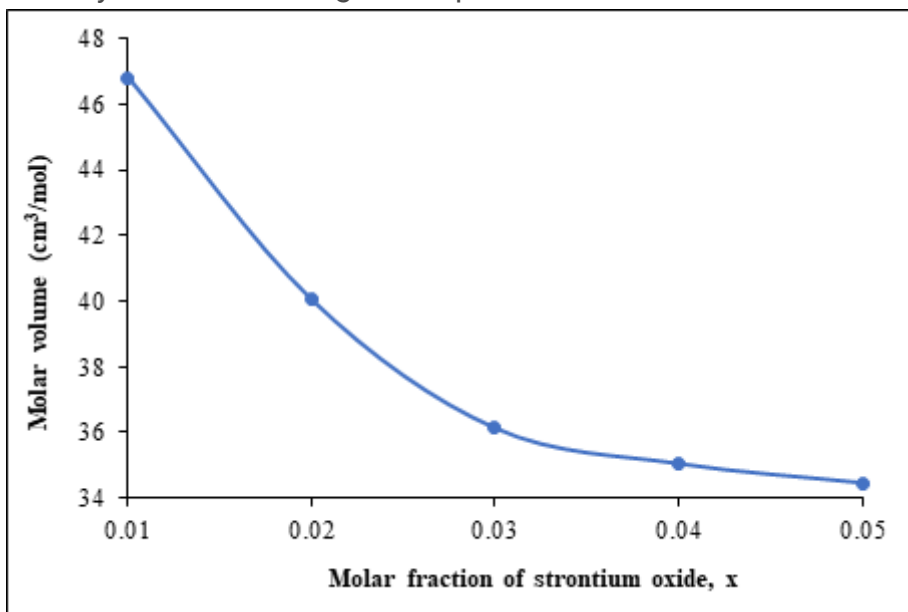


Figure 8

Molar volume of borotellurite glass doped with strontium oxide.

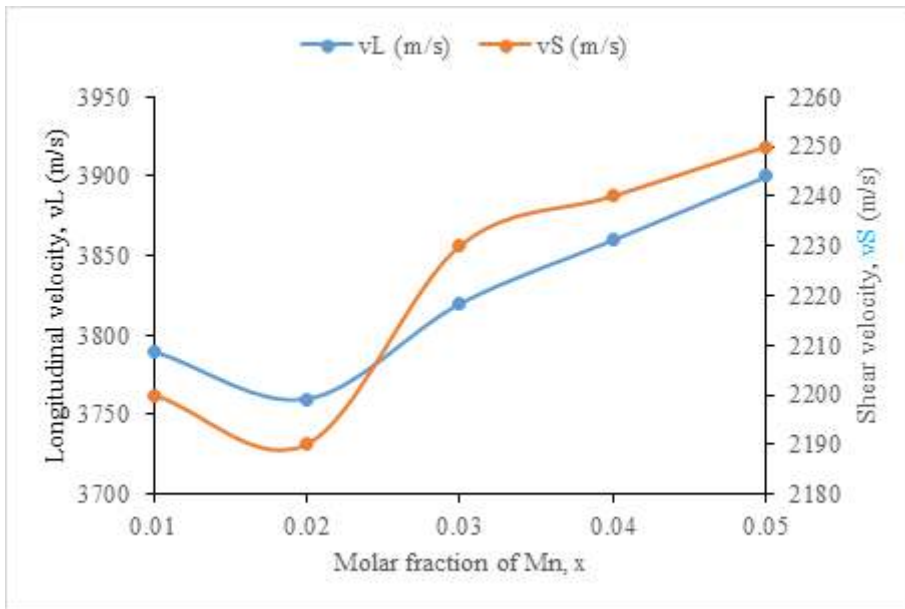


Figure 9

Variation of ultrasonic velocities of borotellurite glass doped with manganese oxide.

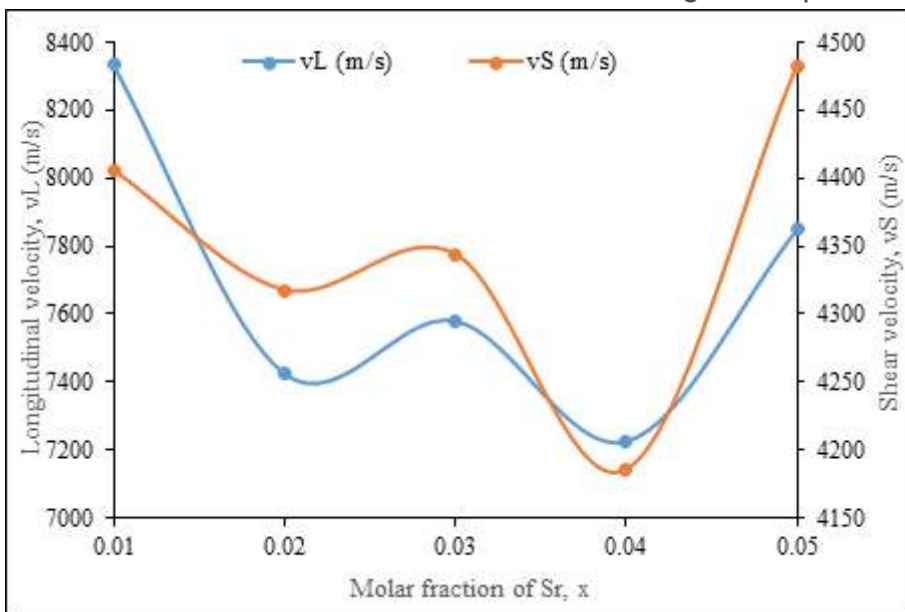


Figure 10

Variation of ultrasonic velocities of borotellurite glass doped with strontium oxide.

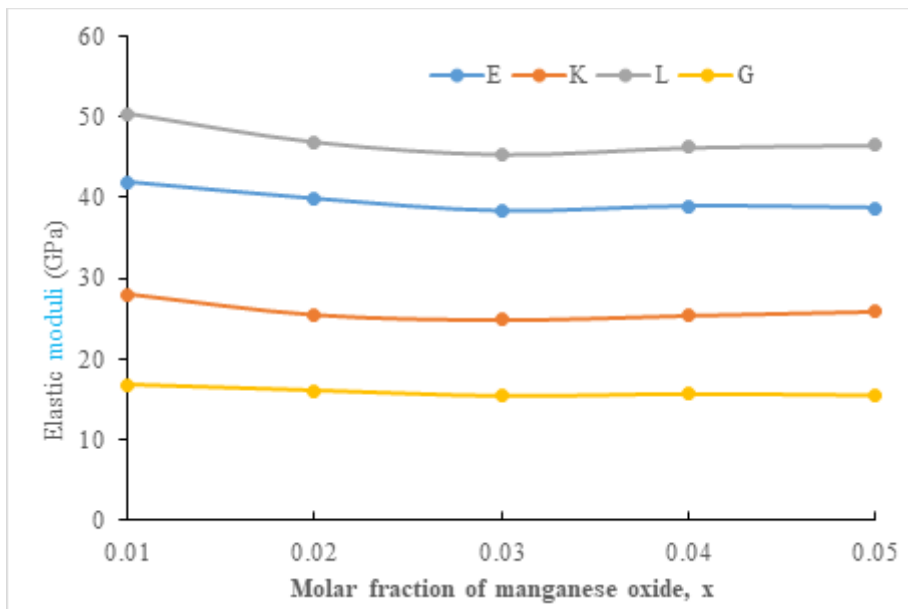


Figure 11

Longitudinal modulus (L), shear modulus (G), Young's modulus (E), and bulk modulus (K) with MnO-2 content for borotellurite glass doped with manganese sample at room temperature.

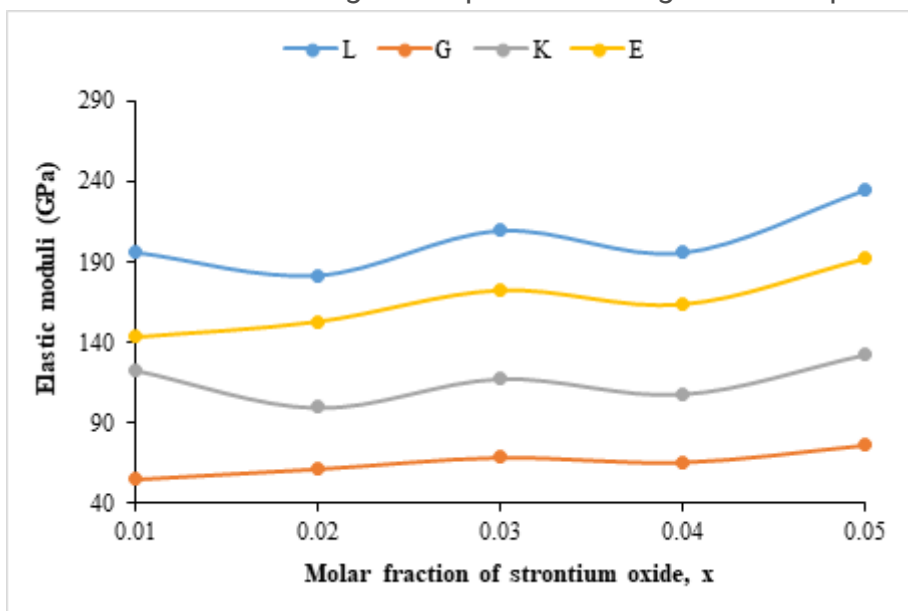


Figure 12

Longitudinal modulus (L), shear modulus (G), Young's modulus (E), and bulk modulus (K) with SrO-2 content for borotellurite glass doped with strontium sample at room temperature.

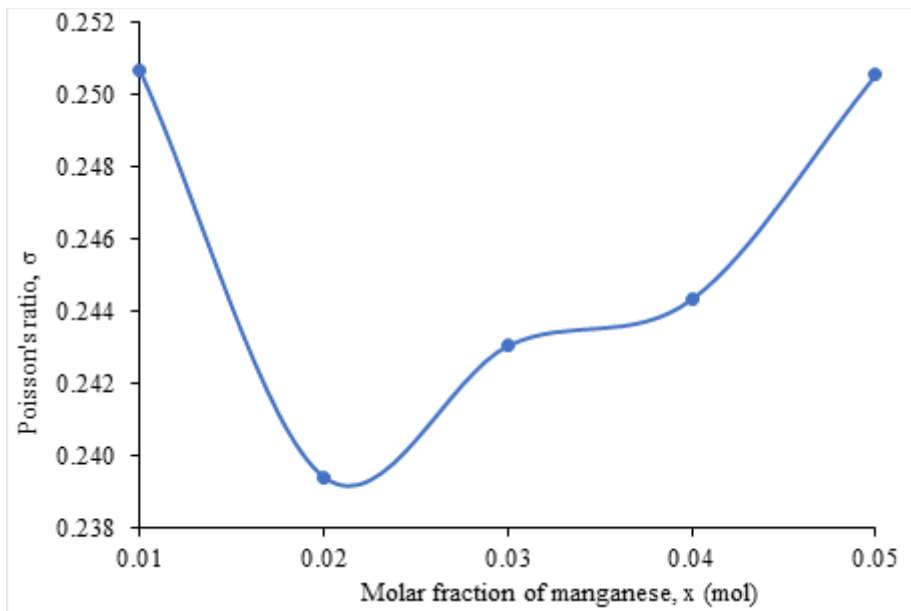


Figure 13

Variation of Poisson's ratio (σ) of borotellurite glass doped with manganese oxide.

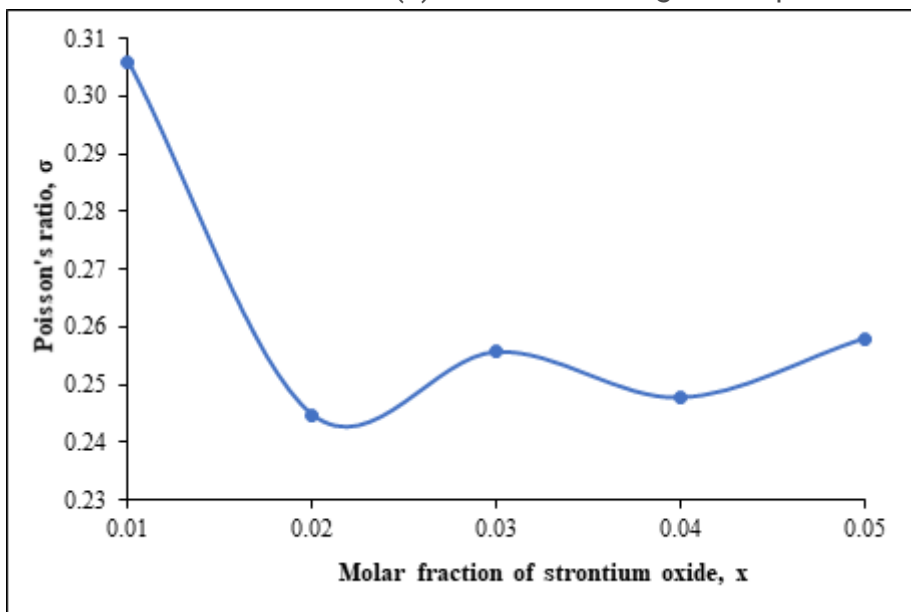


Figure 14

Variation of Poisson's ratio (σ) of borotellurite glass doped with strontium oxide.